Electronic Supplementary Material (ESI) for Nanoscale.


**Supporting Information**

# Virus-templated magnetic composite hydrogels for surface immobilization of mimic-free-lipase

*Wenjing Qi, Huimin Yu**

Department of Chemical Engineering, Tsinghua University, Beijing 100084, P. R. China.

*Correspondence to: Huimin Yu, Department of Chemical Engineering, Tsinghua University, Beijing 100084, China.

Email: yuhm@tsinghua.edu.cn, tel: +8610-62795492, fax: +8610-62770304

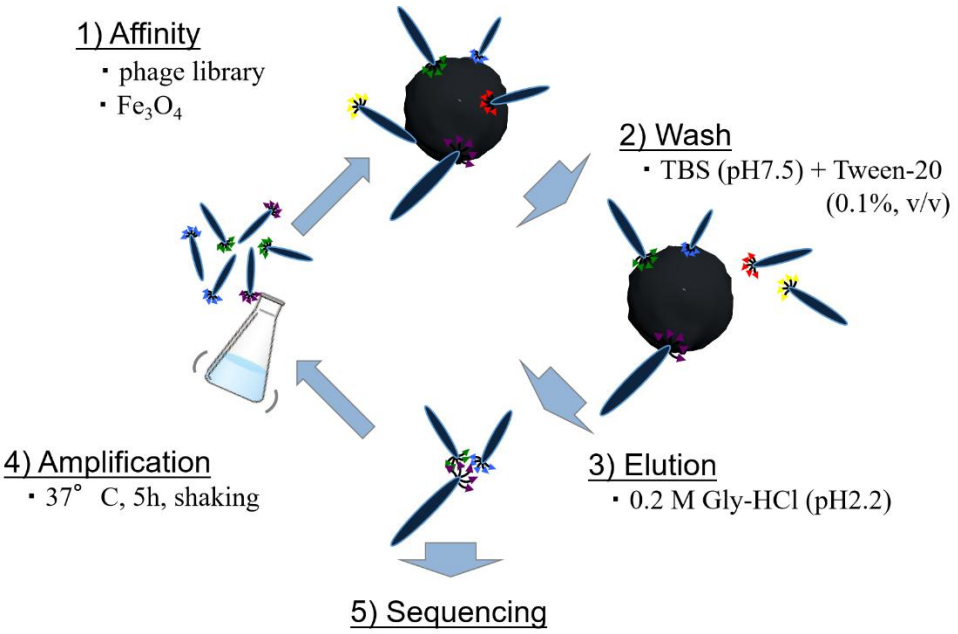


**Fig. S1** Procedure of biopanning for $Fe_3O_4$-specific affinity peptides (FAP)


**Fig. S2** Middle-scale culture procedure of M13 phages. **Step 1:** One single colony of host bacteria ER2738 was cultivated in 20 mL LB liquid culture medium at 37 ℃, 200 rpm for 12h. **Step 2:** $3\times10^{12}$ pfu M13 phages and 1 mL ER2738 seed liquid were inoculated in 100 mL LB/300ml shaking flasks (1 L LB in total) at 37 ℃, 200 rpm for 12h. **Step 3:** The culture medium was centrifuged to remove the cell pellet of bacteria ER2738 at 4 ℃, 8000 rpm for 10 min. **Step 4:** Phages remaining in the supernatant were deposited by adding 1/6 volume of PEG/NaCl solution (20 % (w/v) PEG-8000 and 2.5 M NaCl) and refrigerated for 8h at 4 ℃, **Step 5:** The phages were harvested by centrifuging at 4 ℃, 8000 rpm for 15 min. The solutions with different M13 phage concentration were obtained by resuspension of the pellets in different amounts of deionized water.

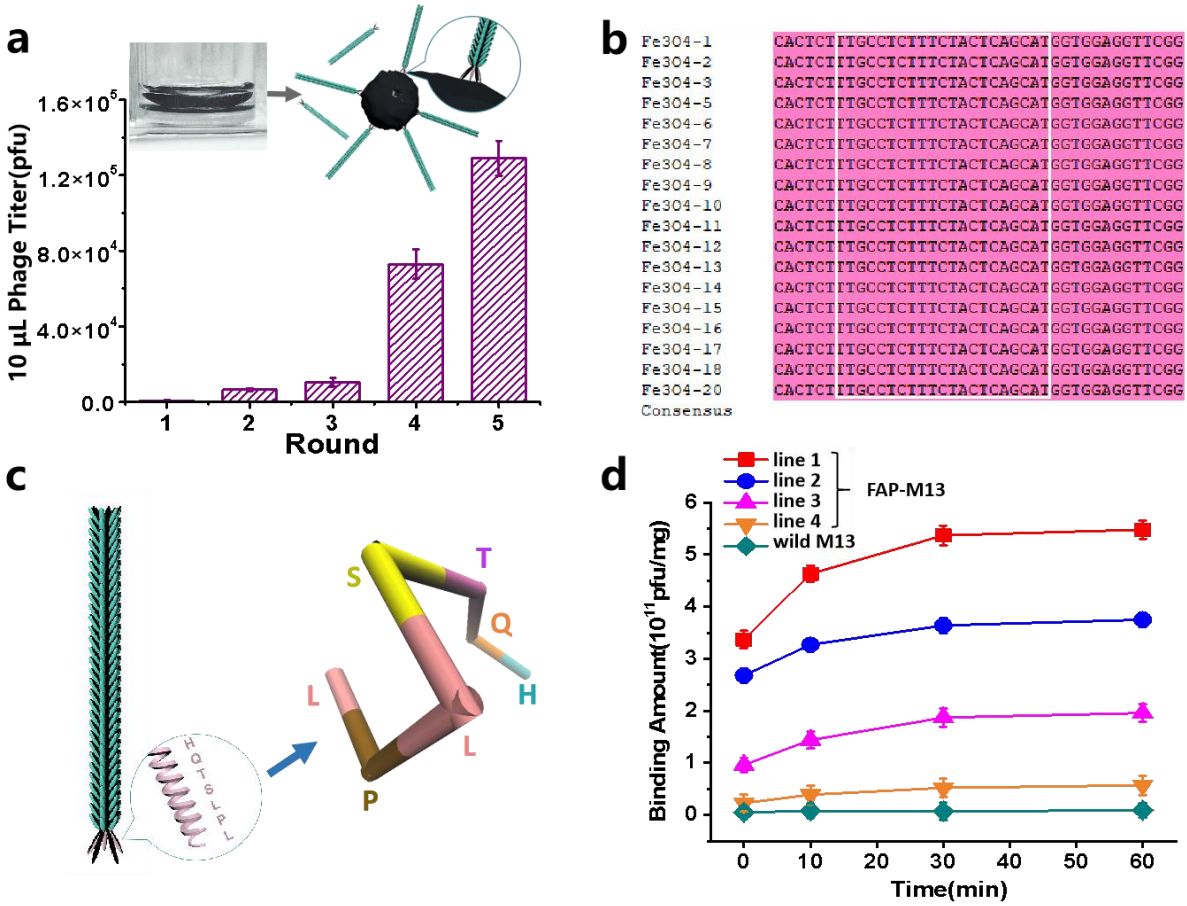


**Fig. S3** Biopanning of FAP-M13 and identification of the FAP peptide. (a) The titer of the binding M13 was enhanced round-by-round from the 1st to 5th cycle of selection. (b) Sequencing result of 20 colonies from the round-5 biopanning, 7-mer amino acid sequences were circled in the white line. (c) Three-dimensional structure of the optimal FAP peptide predicted by the 3Dpro model of Scarch Protein Predictor (http://scratch.proteomics.ics.uci.edu/). (d) Influence of phage concentration and binding time on the binding amount of FAP-M13 with bare $Fe_3O_4$. After mixing $Fe_3O_4$ (0.5 mg, 600 nm) and FAP-M13 phages ($2\times10^{12}$ pfu), the PB buffer was added to obtain varying total volumes (50 μL, 100 μL, 150 μL, and 200 μL), thereby changing the final concentration of FAP-M13 phages (line 1: $4\times10^{13}$ pfu/mL, line 2: $2\times10^{13}$ pfu/mL, line 3: $1.33\times10^{13}$ pfu/mL, line 1: $1\times10^{13}$ pfu/mL). Wild M13 phages ($2\times10^{12}$ pfu, 50 μL) without the special pIII protein were also mixed with $Fe_3O_4$ (0.5 mg, 600 nm) as a control. The

mixture was placed in a metal bath shaker for varied time at 37 ℃, 200 rpm. For one $Fe_3O_4$ particle with diameter of 600 nm, its surface area is about $1.1\times10^6$ $nm^2$ and its mass is about $5.9\times10^{-10}$ mg, thus one $Fe_3O_4$ particle can accommodate theoretical maximum about $3\times10^4$ pfu of FAP-M13 whose cross sectional area is about 33.2 $nm^2$. For the line 1 in Figure 3d, the quantified binding amount was $5.3\times10^{11}$ pfu FAP-M13/mg $Fe_3O_4$, in other words, on a single $Fe_3O_4$ particle, about 318 pfu FAP-M13 were binded. The wild M13 could not attach on the bare $Fe_3O_4$ nanoparticles as FAP-M13 did, and both phage concentration and binding time influenced the binding amount of FAP-M13 towards bare $Fe_3O_4$. The optimal high concentration of FAP-M13 (line 1: $4\times10^{13}$ pfu/mL) was beneficial for the binding, and the optimal binding time was 30 min.

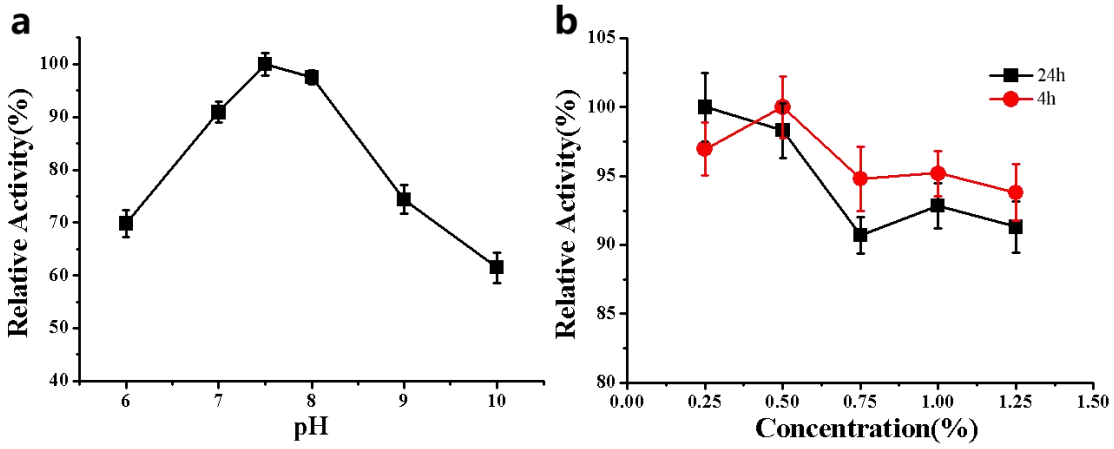


**Fig. S4** Optimization of magnetic composite hydrogel preparation conditions. (a) Optimization of crosslinking pH under 0.5% glutaraldehyde at 37 ℃, 200rpm, 4h. (b) Optimization of glutaraldehyde final concentration for crosslinking under 4h or 24h at pH=7.5, 37 ℃, 200rpm.

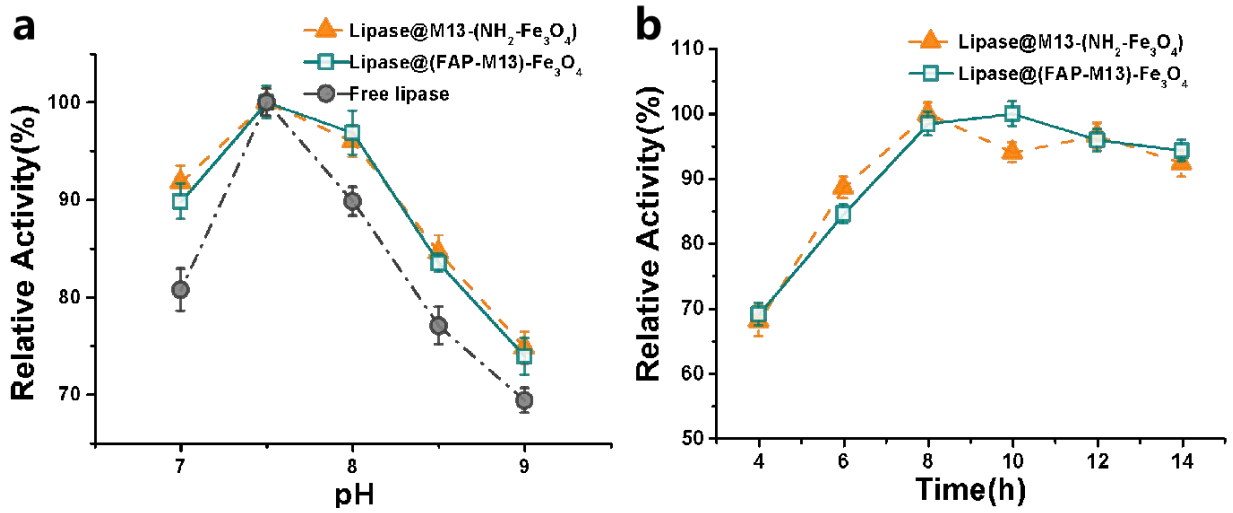


**Fig. S5** Optimization of immobilization conditions. (a) Optimization of immobilization pH. PB buffer of varied pH. 100 μL magnetic carrier and 100 μL lipase (5 mg/mL) were mixed at varied pH. After 12 h of immobilization at 37 ℃, 200 rpm, the immobilized lipase was recovered and the residual activity was measured at 37 ℃, pH=7.5 for 10 min. (b) Optimization of immobilization time at pH=7.5, 37 ℃, 200 rpm.

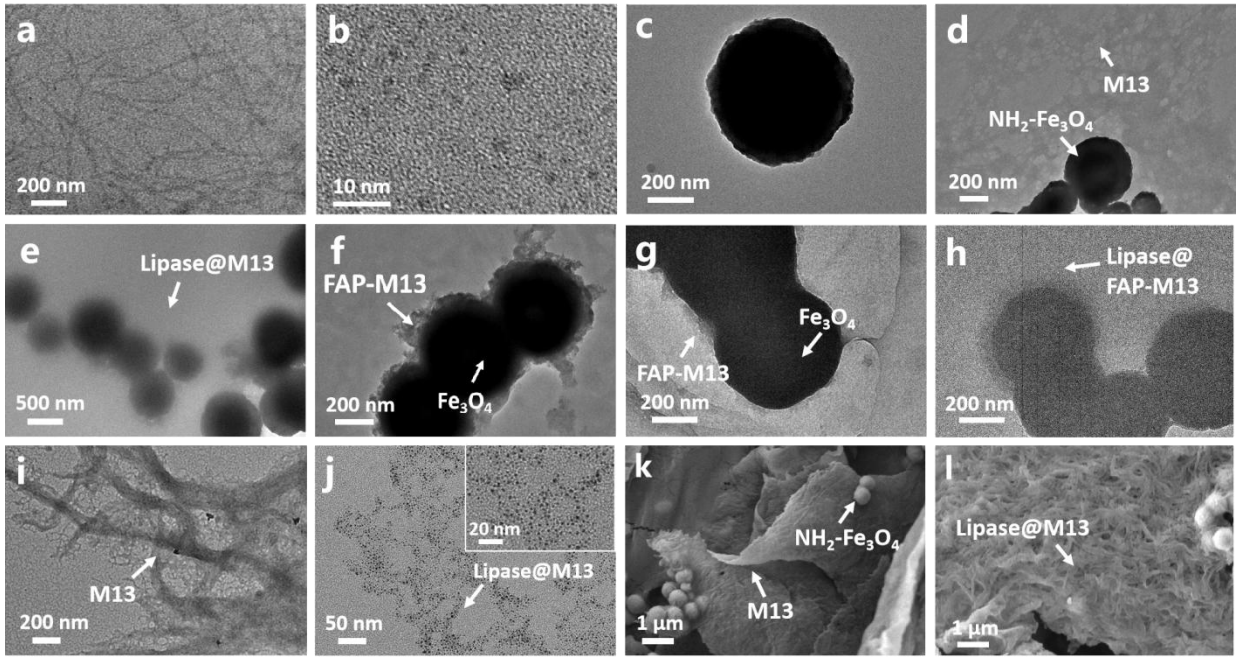


**Fig. S6** The structures of the magnetic virus hydrogels and the MFLs. The TEM images of (a) FAP-M13; (b) lipase; (c) $Fe_3O_4$. Additional representative TEM images of (d) M13-($NH_2$-$Fe_3O_4$), arrows point to crosslinked M13 hydrogel network and $NH_2$-$Fe_3O_4$; (e) lipase@M13-($NH_2$-$Fe_3O_4$), arrow points to lipase@M13 surrounding $NH_2$-$Fe_3O_4$; (f) FAP-M13 affinity binding on $Fe_3O_4$ particle, and high phage concentration of FAP-M13 was used to observe obvious phage gel layer, arrows point to FAP-M13 layer and bare $Fe_3O_4$; (g) (FAP-M13)-$Fe_3O_4$, arrows point to crosslinked FAP-M13 hydrogel network and bare $Fe_3O_4$; (h) lipase@(FAP-M13)-$Fe_3O_4$, arrow points to lipase@FAP-M13 surrounding $Fe_3O_4$. The negative staining TEM images of (i) M13 hydrogel, arrows point to crosslinked M13 hydrogel network; (j) lipase@M13 hydrogel, arrow points to lipase@M13. The SEM images of (k) M13-($NH_2$-$Fe_3O_4$), arrows point to crosslinked M13 hydrogel network and $NH_2$-$Fe_3O_4$; (l) lipase@M13-($NH_2$-$Fe_3O_4$), arrow points to lipase@M13 surrounding $NH_2$-$Fe_3O_4$.

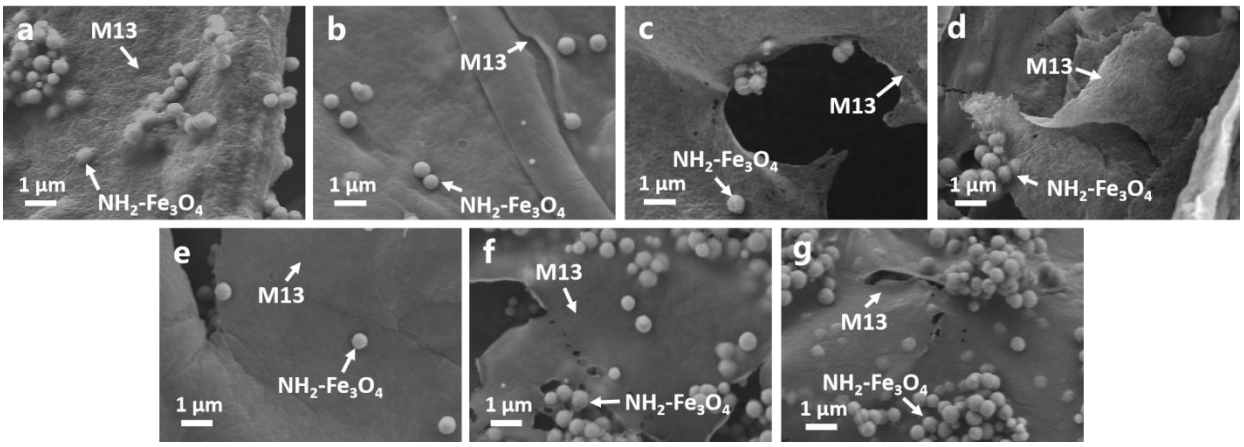


**Fig. S7** The SEM images of the structures of M13-($NH_2$-$Fe_3O_4$) magnetic virus hydrogels under different crosslinking pH including (a) pH = 4, (b) pH = 6, (c) pH = 7, (d) pH = 7.5, (e) pH = 8, (f) pH = 9, (g) pH = 11. The rest of preparation conditions were 0.5% glutaraldehyde at 37 ℃, 200rpm, 4h. Arrows point to crosslinked M13 hydrogel network and $NH_2$-$Fe_3O_4$.

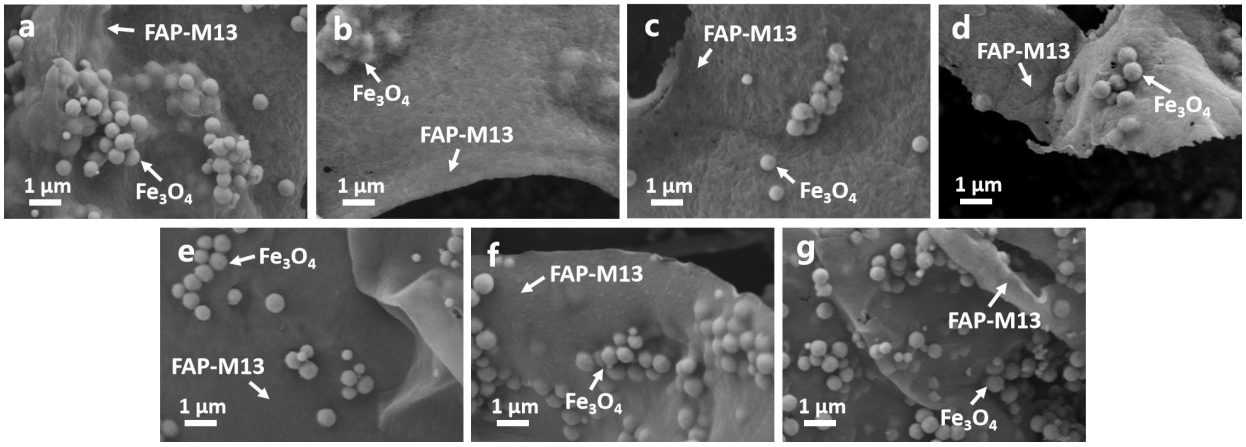


**Fig. S8** The SEM images of the structures of (FAP-M13)-$Fe_3O_4$ magnetic virus hydrogels under different crosslinking pH including (a) pH = 4, (b) pH = 6, (c) pH = 7, (d) pH = 7.5, (e) pH = 8, (f) pH = 9, (g) pH = 11. The rest of preparation conditions were 0.5% glutaraldehyde at 37 ℃, 200rpm, 4h. Arrows point to crosslinked FAP-M13 hydrogel network and bare $Fe_3O_4$.

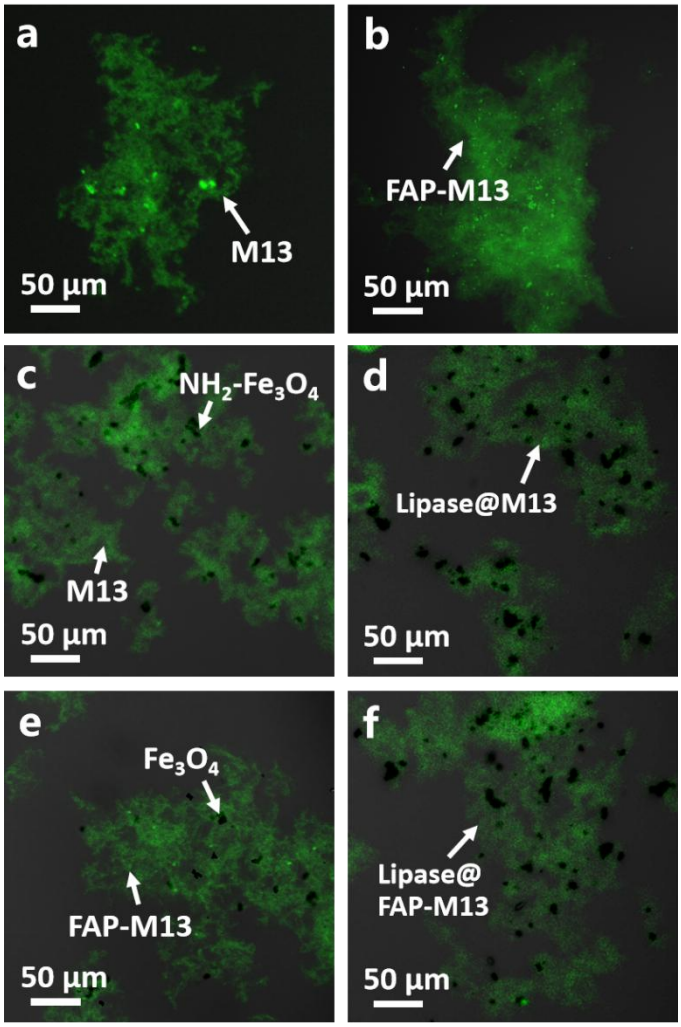


**Fig. S9** The structures of the magnetic virus hydrogels and the MFLs. The confocal laser scanning microscopy (CLSM) images of (a) M13 hydrogel, arrow points to crosslinked M13 hydrogel network; (b) FAP-M13 hydrogel, arrow points to crosslinked FAP-M13 hydrogel network; (c) M13-($NH_2$-$Fe_3O_4$), arrows point to crosslinked M13 hydrogel network and $NH_2$-$Fe_3O_4$; (d) lipase@M13-($NH_2$-$Fe_3O_4$), arrow points to lipase@M13 surrounding $NH_2$-$Fe_3O_4$; (e) (FAP-M13)-$Fe_3O_4$, arrows point to crosslinked FAP-M13 hydrogel network and bare $Fe_3O_4$; (f) lipase@(FAP-M13)-$Fe_3O_4$, arrow points to lipase@FAP-M13 surrounding $Fe_3O_4$. The autofluorescence of the hydrogels and the MFLs was the result of the reactions between proteins (phages and lipases) and glutaraldehyde.

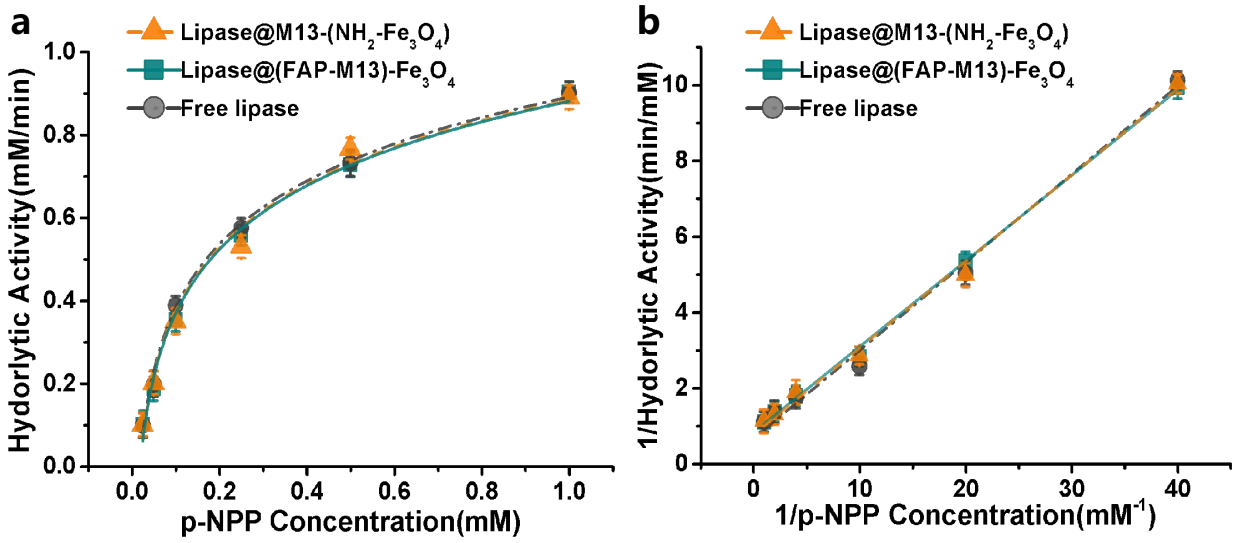


**Fig. S10** Michaelis-Menten plots of the MFLs and free lipase. (a) Hydrolytic activity of free lipase and immobilized lipase at varied p-NPP concentration. (b) Michaelis-Menten kinetics evaluated through Lineweaver Burk plots.